Technical Note: Semi-rigid chambers for methane gas flux measurements on tree stems

A. Siegenthaler[1*], B. Welch[1], S. R. Pangala[1], M. Peacock[1], V. Gauci[1]

[1] {Centre for Earth, Planetary, Space & Astronomical Research, Department of Environment, Earth & Ecosystems, The Open University, Milton Keynes, UK}

*Correspondence to: A. Siegenthaler (andy.siegenthaler@alumni.epfl.ch)

Abstract

There is increasing interest in the measurement of methane (CH_4) emissions from tree stems in a wide range of ecosystems so as to determine how they contribute to the total ecosystem flux. To date, tree CH_4 fluxes are commonly measured using rigid closed chambers (static or dynamic), which often pose challenges as these are bulky and limit measurement of CH_4 fluxes to only a very narrow range of tree stem sizes and shapes. To overcome these challenges we aimed to design and test new semi-rigid stem-flux chambers (or sleeves). We compared the CH_4 permeability of the new semi-rigid chambers with that of the traditional rigid chamber approach, in the laboratory and in the field, with continuous flow or syringe injections. We found that the semi-rigid chambers had reduced gas permeability and optimal stem gas exchange surface to total chamber volume ratio (Sc/Vtot) allowing better headspace mixing, especially when connected in a dynamic mode to a continuous flow gas analyser. Semi-rigid sleeves can easily be constructed and transported in multiple sizes, are extremely

light, cheap to build and fast to deploy. This makes them ideal for use in remote ecosystems where access logistics is complicated.

1 Introduction

Recent research into ecosystem greenhouse gas fluxes has shown that tree stems emit significant amounts of methane (CH_4) (Terazawa et al., 2007; Rusch and Rennenberg, 1998; Gauci et al., 2010; Pangala et al., 2013; Rice et al., 2010; Terazawa et al., 2015) although the transport mechanisms and global importance of tree-mediated emissions remain largely unknown. These past investigations have used a variety of closed chambers adapted to various tree-stem sizes. Presently, the most common chambers used to measure CH_4 emissions from tree-stems are closed rigid chambers in the form of either a vertical cylinder, a horizontal cylinder or a cube fitted around tree-stems (e.g. Gauci et al., 2010; Pangala et al., 2013; Terazawa et al., 2007; Hari et al., 1991; Rusch and Rennenberg, 1998). These chambers can be deployed either vertically by enclosing the whole stem or, alternatively when the stems are too large, laterally on the stem, covering only a small fraction of the stem surface (e.g. Levy et al., 1999; Teskey and McGuire, 2005; Ryan, 1990; Hari et al., 1991). These techniques were originally designed to measure CH_4 and carbon dioxide (CO_2) from samples manually taken with syringes and analysed by gas chromatography. The ratio between the gas exchange surface and the chamber volume (S_c/V_{tot}) was transposed from soil chambers and were not necessarily adapted to the lower fluxes found in tree-stems, and are therefore often too high (Hutchinson and Livingston, 2001). In other words, if the chambers are too large for a given exchange surface, mixing problems may occur, making it important to circulate the air in their headspace (Hutchinson and Livingston, 1993; Rusch and Rennenberg, 1998).

With the advent of continuous flow analytical techniques and increasing precision of instruments (e.g. cavity ring-down spectroscopy, infrared and photo-acoustic gas analysers), the need for longer accumulation periods to detect significant concentration changes has become obsolete. The tendency is to reduce the accumulation period as much as possible in order to be able to use more straightforward linear regressions to determine fluxes closest to the point of chamber closure. Unlike open chamber techniques which allow steady state measurements (e.g. Bortoluzzi et al., 2006; Norman et al., 1997; Subke et al., 2003; Pumpanen et al., 2004), closed chambers are non-steady state systems; the diffusive laws advocate the use of non-linear regressions of gas concentrations as a function of time to determine rates, as these decrease with increasing gas saturation (Hutchinson and Livingston, 2001; Pihlatie et al., 2013; Pumpanen et al., 2004; Kutzbach et al., 2007).

With continuous flow gas analysers there are three main advantages: 1) they are non-dispersive as no gas needs to be taken out of the measurement system and irreversibly "consumed", 2) they circulate air between the chamber and the gas detectors, which for small chamber volumes could represent enough mixing to avoid underestimations of fluxes by as much as 36 to 58% in non-mixed soil-atmosphere exchanges (Christiansen et al., 2011), and 3) with measurement frequencies of up to 10 Hertz and precisions of ±2 ppb the closure time needed to get a representative accumulation slope has been dramatically reduced using these devices (excluding the equilibration period) and therefore it also avoids underestimations due to regressions made over longer periods of time (Hutchinson and Livingston, 2001; Pihlatie et al., 2013). In addition, recent work has focused on trace gases (e.g. CH_4 and N_2O) which have lower accumulation rates compared to the more frequently measured CO_2 (IPCC, 2007), moderating the saturation issue inherent to non-steady state setups (Hutchinson and Livingston, 2001). Altogether, these point towards the use of a smaller stem chamber with larger gas exchange surface per chamber volume proportion (Sc-to-Vtot ratio).

A further complicating factor is field access. Stem-methane emissions have recently begun to be investigated in remote areas such as in forested tropical wetlands with often no road access. In those areas it is a logistical challenge to carry large/heavy loads. Moreover, because of the great variety of stem sizes/shapes, a whole collection of rigid chambers is usually needed to cover most of the ecosystem tree species thus creating further logistical and cost issues.

In order to meet the new challenges presented by the growing interest in measuring greenhouse gas fluxes from tree-stems we aimed to design, describe and test/deploy new semi-rigid stem-emission chambers in the laboratory and in the field, and to compare their permeability to CH_4 (gas conductance) with previously described rigid chambers. Thus far, semi-rigid sleeve chambers have been used effectively in several of our measurement campaigns. We therefore consider their detailed reporting to be of interest to a broader constituency of eco-physiologists and biogeochemists. We also examine various methodological benefits and logistical advantages of using this new approach.

2 Materials and methods

2.1 Chamber designs: semi-rigid sleeve and rigid chamber

Our approach to measure stem CH_4 emissions, which could also include other greenhouse gases produced in anaerobic conditions such as N_2O, uses a semi-rigid chamber (or sleeve). The preferred material was a pre-shaped and gas impermeable PET (polyethylene terephthalate) or PC (polycarbonate) plastic sheet with a natural tendency to curve induced by 3-4 vertically distributed imprinted rims on the periphery. These rims ensured good stability and helped maintain the desired natural curvature of the sleeve that proved to be very helpful for the deployment of the sleeves on the stems as the sleeve could hold in place without straps.

94 To investigate permeability changes due to both the size and the approach, we used two semi-
95 rigid sleeves together with a rigid chamber. As this was straightforward, for the smaller semi-
96 rigid sleeve we sourced the pre-shaped material from a cylindrical 3 L soft drink bottle, which
97 already had the desired imprinted rims. The 0.1 mm thick bottle was truncated above and
98 below the cylindrical section, and opened vertically on the side. For the larger sleeve we
99 sourced the material from 0.2 mm thick not pre-shaped semi-rigid PC sheets. Both types of
100 plastic sheets have very low gas permeabilities under experimental standard ambient
101 temperature and pressure (SATP from UIPAC) conditions and short chamber enclosure times
102 (McKeen, 2012).

103 The edges of the sheets were framed with 1.5 cm thick and 3 cm wide adhesive backed
104 expanded Neoprene strips (Seals+Direct Ltd, Hamphshire, UK); closed cell neoprene foam
105 that is gas tight and can be bent, but is hardly compressible (≤ 3 % with 200 N). This
106 Neoprene strip was placed as a frame around the rectangular sheet to provide a seal and to
107 ensure a constant volume between the sheet and the tree stem (Fig. 1). The adhesive was
108 provided on one side of the expanded Neoprene strips. Inside this framed volume we placed
109 two Neoprene vertical wedges (1.5 cm thick and 3 cm wide) to keep the sheet equidistant
110 from the stem all along the radial periphery of the sleeve. The sleeve was also equipped with
111 two snap-on rubber caps with inserted three-way Luer-lock stopcocks (BBraun, Bethlehem,
112 USA) that permitted connection to the Ultraportable Greenhouse Gas Analyser (UGGA, Los
113 Gatos Research Inc., Mountain View, USA) via two 4.6 m long and 5 mm inside diameter
114 PTFE (polytetrafluoroethylene) coated PVC (polyvinyl chloride) parallel tubes (Nalgene,
115 Rochester, USA). As venting was recommended (Hutchinson and Livingston, 2001;
116 Christiansen et al., 2011) both sleeves were equipped with a coiled vent tube (18 cm long, 1.2
117 mm inner diameter). We downscaled the vent described by Hutchinson and Livingston (2001)
118 by a factor 48 in terms of vent volume whereas the sleeves were a factor 10 to 20 less

119 voluminous as compared to the authors' chamber (14 L). Their study showed that in a
120 perfectly sealed chamber, after 30 minutes of deployment the gas mass loss through the sole
121 vent represented 0.038% of the target gas.

122 We tested all the components of the semi-rigid sleeves independently for unwanted
123 background contaminations that could interfere with CH_4 emissions from the stems by
124 incubating them for two hours in 500 mL borosilicate glass beakers filled with air and
125 connected in continuous flow with the UGGA. The selected raw material was inert and did
126 not interfere with measurements from the environment. We also tested the compressibility of
127 sleeves by pulling the straps with a 200 N force (twice 100N) and measuring the thickness of
128 the Neoprene frame before and after pulling (Fig. 2, see also chamber deployment section).

129 We also compared the CH_4 losses from our new semi-rigid sleeves with a previously used
130 rigid chamber design, similar to the ones constructed and described in other studies (Rusch
131 and Rennenberg, 1998; Gauci et al., 2010; Pangala et al., 2013). The closed rigid chamber
132 was constructed from cylindrical Perspex® (Perspex, Tamworth, UK) of inner diameter of 28
133 cm and had an inner height of 30 cm. The cylinder was cut into two halves, which were held
134 together with a metal hinge. The two half-cylinders were framed within a 5 cm wide and 1 cm
135 thick frame made of flat Perspex® that was fitted with Neoprene strips. The cylindrical
136 chamber had a central opening to enclose the tree stem. Two smaller cylinders (18 cm
137 diameter x 5 cm height) were attached on either side of that opening (Fig. 3). The chamber
138 was equipped with a gas sampling port and a small vent tube (12 cm long; 6 mm diameter).

139

140 ## 2.2 Enclosed chamber volume and gas exchange surface determinations

141 The volume of the semi-rigid sleeves could be determined precisely in two different ways.
142 Firstly, we extrapolated the empirical total chamber volume (V'_{tot}) from the CH_4

concentration dilution factor after having inserted a known volume ($V_{standard}$) of a 2000 ppmv CH_4 standard (Air Liquide, Paris, France) into the sleeve's enclosed volume and measuring the end concentration (C_0) after dilution, and subtracting the atmospheric CH_4 concentration (C_{atm}) originally in the chamber. The two semi-rigid sleeves and a rigid chamber were attached to an inert stainless steel cylinder (see chamber deployment). The dilution was done in 90 seconds so that the losses through gas permeability of the chambers remained negligible. This extrapolation was formalised as:

$$V'_{tot} = V_{standard} * \frac{(C_{standard})}{(C_0 - C_{atm})} \quad (1)$$

Secondly, we also calculated the theoretical volume of the sleeves (V_c) by subtracting a sector (K) of both, a smaller cylinder volume (V_{stem}) from a larger cylinder volume (V_{ext}), minus the volume taken by the vertical wedges (V_{wedges}) (Fig. 4). The sector (K) was determined from a ratio between the sleeve length (L) and the circumference at the external edge of the sleeve (πD_{ext}). The sleeve length (L) is the length of the incompressible external edge of the chamber and represents a fraction of the total circumference given by πD_{ext}. The diameter of the smaller cylinder (the compressible internal foamy edge) is given by the diameter of the stem (D_{stem}). The larger cylinder diameter (D_{ext}) is the diameter given by the stem (D_{stem}) plus the thickness (T) of the sleeve. Both cylinders have the same height (H). Thereafter, we have:

$$D_{ext} = D_{stem} + 2T \quad (2)$$

$$K = \frac{L}{\pi D_{ext}} = \frac{L}{\pi(D_{stem}+2T)} \quad (3)$$

$$V_C = K(V_{ext} - V_{stem}) - V_{wedges} = \frac{HL}{(D_{stem}+2T)} * \left[\left(\frac{D_{stem}+2T}{2}\right)^2 - \left(\frac{D_{stem}}{2}\right)^2\right] - V_{wedges} \quad (4)$$

However, the total volume (V_{tot}) is the sum of the chamber volume (V_c) plus the dead volume enclosed in the gas analyser and the tubes (V_{dead}):

$$V_{tot} = V_C + V_{dead} \quad (5)$$

Similarly, the gas exchange surface of the sleeves (S_c) was calculated by considering the sector (K) of the stem surface (S_{stem}) covered by the chamber at the circumference of the stem (πD_{stem}) and the height of the sleeve (H), minus the small surface covered by the vertical wedges (S_{wedges}):

$$S_c = K * S_{stem} - S_{wedges} = \frac{HL}{(D_{stem}+2T)} * D_{stem} - S_{wedges} \quad (6)$$

2.3 Chamber deployment

The three types of chambers (two semi-rigid sleeves and one rigid chamber) were deployed on a gas-inert stainless steel cylinder of diameter 15 cm. The semi-rigid chambers were flattened around the cylinder and subsequently attached and tightened with two metal cam straps at the top and bottom of the frame (Figure 2). The straps were 1.5 m long and 3 cm wide. An additional strap was necessary at mid-height of the bigger sleeve to ensure a good cohesion of the vertical Neoprene frames and vertical wedges with the stem (steel cylinder in this case).

Before installing the rigid acrylic chamber, closed cell Neoprene foam bands (7 cm wide and 4 cm thick) were attached at the bottom of the inert stainless steel cylinder and also at 35 cm height using double-sided Scotch tape (3M, St-Paul, USA) to append the extremities of the band as well as packing brown tape (5 cm wide) to tighten the band firmly against the metallic cylinder. The two mobile panels of the chamber were opened and the upper and lower half-necks of one panel were lodged around the two foam bands by compressing the foam so as to ensure gas tightness. Finally, all open-end flanges surrounding the cylindrical volume were progressively closed with Handy-grips (Irwin, Vernier, Switzerland).

We used the larger semi-rigid chamber to exemplify the field deployment (Table 1). We deployed it on twelve tree-stems (diameter at breast height: 25-45 cm) located in the northern boreal zone (*Pinus sylvestris* and *Betula pendula*, Degerö mire, Sweden) as well as in a tropical lowland forest (*Heisteria concinna,* Barro Colorado Island, Panama). The sleeves were placed at mid-height on the stems at 35 cm of height. We shaded the sleeves with a plasticised aluminum foil to minimise any changes to chamber temperature which might otherwise affect stem-gas exchange processes. In the lab this measure was unnecessary. We tested the sleeve's CH_4 concentration change on both, very smooth birch stems and very rough pine-tree stems to contrast the concentration readings as much as possible. To ensure optimal gas tightness it was important to distribute the pressure of each strap all around the surface of the sleeve. We visually checked for gaps between the stem and the Neoprene strips. Monitoring the CH_4 concentration change in a continuous flow mode made an optimal gas tightness test. A leaking chamber (mainly pressure-driven bulk flow following Hagen-Poiseuille's law) typically displayed fluctuating concentrations with concentration build-up being recurrently drawn down. Finally, we also used the larger semi-rigid sleeve together with a manual syringe sampling. For that purpose we used a 30 mL plastic syringe fitted with a Luer-lock three-way stopcock (BBraun, Bethlehem, USA) and connected it to one of the two stopcocks on the sleeve. At t=0, t=5, t=10 and t=15 minutes we collected 12 mL of gas sample from the sleeve and transferred it into pre-evacuated glass Exetainers (Labco Ltd, Ceredigion, UK) before analysing CH_4 concentrations on a Fast Methane Analyser (Los Gatos Research Inc., Mountain View, USA) equipped with a sampling loop as described in Baird et al. (2010).

2.4 Gas Analyses

For the permeability tests, the CH_4 concentration change was analysed in the laboratory under SATP conditions for three types of chamber (Table 1, Supplement S1); a rigid chamber and two semi-rigid sleeves. We injected 50 mL of a 2000 ppmv methane standard (Air Liquide, Paris) into these chambers after which the CH_4 concentration decline was measured over 20 minutes in continuous flow mode. Each chamber type was tested in triplicate. For the blanks, we injected ambient air. The slopes were measured from a linear regression of declining concentrations starting after an equilibration time of 90 seconds (dead band) and running for 20 min. This dead band represents a maximum time for the continuous flow circuit to mix the entire headspace (V_{tot}).

In the field, the CH_4 concentration changes of a larger sleeve were monitored when deployed on various tree-stem species (see chamber deployment). In order to have a set of contrasting responses we selected, a posteriori, measurement runs with both high and low rates, and also included runs where leakages of the sleeve were present (Figs. 5 and 6, Supplements S3 and S4). Methane concentration accumulations were measured as in the laboratory although with shorter runs of approximately 420 seconds. In the manual sampling mode with syringe, the accumulation period was 900 seconds. The slopes were measured from linear, quadratic and exponential regressions of increasing concentrations starting after a dead band of 90 seconds. The gas pressure, temperature and humidity inside the stem sleeve were measured from the circulated gas running through the UGGA's flow-cell and we used temperature, pressure and humidity compensated CH_4 concentrations for the slope calculations. The advantage of using the cell temperature is the perfect synchronicity of the airflow with the temperature measurement. In previous tests we showed that the cell temperature was strongly correlated (R^2 = 0.994) to the chamber temperature measured with a small data logger (ST-171, Clas Ohlson, Insjön, Sweden). Besides, the analytical laser did not significantly increase the temperature of the closed circuit (cell, connection tubes and chamber), as the temperature drift

over 20 minutes of enclosure was only +0.7 % under lab conditions (SATP). The chamber pressure was equilibrated to the outside monitored atmospheric pressure (Gas pressure sensor, Vernier, Beaverton, USA) via the vent tube.

All chambers were connected to an UGGA via two flexible tubes (see chamber designs section) set in parallel in a continuous flow mode; one tube bringing air from the gas analyser towards the chambers and the other tube pumping air from the headspaces towards the gas analyser. The tubes were connected to the gas analyser via two ¼ inch push-connect fittings. The UGGA's pump ensured a continuous flow of 2-4 L min^{-1}. The UGGA measured CH_4 with the Off-Axis Integrated Cavity Output Spectroscopy (OA-ICOS) at a frequency of 0.33 Hz. The analyser's uncertainty in the range of 0.01 ppmv to 100 ppmv of methane is <1% without calibration and the precision is ±0.6 ppb over a period of 100 seconds (LGR, 2013).

2.5 Methane permeability calculations

In order to quantify and compare CH_4 losses from the three types of chambers (two semi-rigid sleeves and one rigid chamber) attached to an inert stainless steel cylinder we corrected the loss rates by taking into account both the stem exchange surface covered by each sleeve (or chamber) as well as the concentration gradient between inside and outside of each chamber. To express this we calculated the permeability as a function of the effluxes (outgoing fluxes) and the concentration gradient between inside and outside the chambers.

In the first step we multiplied the slope (mg m^{-3} s^{-1}) by the total volume of the chamber (V_{tot}) to get the loss rates (mg s^{-1}). We then divided the loss rates from each sleeve (or chamber) by the stem exchange surface (S_c) covered by each sleeve (or chamber) to express the methane flux (J) which can be used for both the permeability experiment on the metallic cylinder and the methane accumulation runs from tree-stems in the field:

$$Loss\ rate = slope * V_{tot} = \frac{dC}{dt} * V_{tot}\left[\frac{mg}{s}\right] \quad (7)$$

$$Flux\ (J) = \frac{Loss\ rate}{S_c} = \frac{dC}{dt} * \frac{V_{tot}}{S_c} \left[\frac{mg}{m^2 s}\right] \quad (8)$$

In the second step, from Fick's first law (Fick, 1855) we could apply the general equation often used in cell biological or textile fabric applications (Ogulata and Mavruz, 2010) to calculate, for each sleeve (or chamber), the CH_4 permeability (P) through a porous medium by dividing the CH_4 flux (J) by the CH_4 concentration gradient (ΔC) between inside ($C_{chamber}$) and outside of the sleeve (C_{atm}). We assume that the diffusive CH_4 losses (including dilutions) through the rigid and semi-rigid material are negligible at SATP conditions (McKeen, 2012). Thereafter the equation was:

$$J = -P * \Delta C \rightarrow Permeability\ (P) = -\frac{J}{(C_{chamber} - C_{atm})} \left[\frac{m^3}{m^2 s}\right] \quad (9)$$

2.6 Numerical analyses

We used linear, quadratic and exponential regressions to fit the CH_4 concentrations as a function of the accumulation time in the chambers. The fitting was based on sum of squares' minimisation of the errors. The frequency distribution, homogeneity and homoscedacity of the residuals were previously checked using normal quartile plots, residual versus predicted plots, and box plots. The coefficient of determination (R^2) was used to quantify the level of fit. All the data was analysed with the SAS software (SAS Institute Inc., Toronto, Canada).

3 Results

3.1 Calibration of the semi-rigid sleeves

The compared predicted (theoretical) and the mean observed empirical V'_{tot} (Eqs. 1 and 4) were respectively: 966 and 933 cm^3 for the small sleeve, 1406 and 1439 cm^3 for the large sleeve, and 13581 and 13026 cm^3 for the rigid chamber (Supplement S1). The observed V'_{tot} values included variability due to the possible but very tiny compaction of the Neoprene foam over the whole frame. This compaction was less than 3% of V_{tot}, which was a maximum considering the pulling force of 200 N applied on the straps (twice 100N).

The difference between the mean observed V'_{tot} and the predicted V_{tot} values gave us an estimate of the bias in size. By dividing the absolute value of the bias through the predicted value we get an estimate of the inaccuracy of V_{tot} (chamber, tubes and detector's cell). As all terms of the fraction (Eq. 4) are linearly dependent, the inaccuracy of the permeability (P) is the quadratic mean of all other terms (Table 1, footnote). The gas exchange surface (S_c) could be precisely determined and we assume that there is no error associated with it. The inaccuracies in the concentration measurements are dependent on the uncertainty of the UGGA, which in our case was <1% for the un-calibrated device.

The precision of our measurement system, related to repeatability, is the level to which repeated measurements show the same results under the same conditions. For each sleeve or chamber we repeatedly injected 50 mL of a 200 ppmv standard and measured the initial concentration (C_0, Table 1, Supplement S1) in the enclosed volume. We used the relative standard error (RSE) of the initial concentration (C_o) to express the level of precision between different types of chambers. Thereafter, precision is of ±1.82% for the small sleeve, ±1.59% for the large sleeve and ±1.68% for the rigid chamber.

3.2 Chamber permeability comparisons

The comparison of permeability (Table 1, Supplement S1) of the three types of chamber shows that the semi-rigid sleeves are on average less permeable than the rigid chamber, and that the smaller semi-rigid sleeve had a higher permeability compared to the larger one. It was also interesting to note that the CH_4 loss (negative slope) is lower for the rigid chamber compared to semi-rigid sleeves. The contrasting higher permeability of the rigid chamber was counterbalanced by the much greater V_{tot} as well as a much lower initial concentration gradient between inside and outside of the chamber ($dC = C_0 – C_{atm}$). The rigid chamber was 14.1 times that of the small sleeve in volume and 9.7 times that of a large sleeve, and the initial concentration gradient in the rigid chamber was only 1/14 of that in the smaller sleeve and 1/9 of that in the bigger sleeve. Moreover, the larger sleeve had a larger S_c-to-V_{tot} ratio (0.42) compared to the smaller sleeve (0.34).

In order to understand why the permeability of the semi-rigid sleeves was lower than that of the rigid chamber we compared and calculated the potential contact distances between air from inside and outside of the chamber volumes (Fig. 3, Supplement 2). Those contact zones represented the paths where gas effusion could occur, which were driven by the architecture of the chamber. For that purpose we distinguished two types of contact lines: 1) mobile lines that needed to be sealed properly every time the chambers were deployed and from which most of the losses were likely to occur, and 2) fixed lines that resulted from the manufacture which could be cracked and leak as a result of twisting forces on the rigid joints. The result was that for the same theoretical stem gas exchange surface (S_c) between the two chambers (same length and height), the ratio between the length of the mobile lines and the stem gas exchange surface (S_c) was 2.17x smaller for the semi-rigid as compared to the rigid approach.

3.3 Stem-methane emissions and field deployments

329 In the field, the manual sampling by syringe showed steady concentration changes with the
330 sleeve technique (Fig. 5, Supplement S3), and the linear fitting of those concentration changes
331 was always high ($R^2 \geq 0.924$). When applying a quadratic fit the coefficient of determination
332 improved substantially ($R^2 \geq 0.995$). In continuous flow mode the concentration changes were
333 also consistent with the sleeve technique (Fig. 6, Supplement S4), and the linear fitting was
334 very high ($R^2 \geq 0.989$) for all the runs not displaying leakages. Equally to the manual sampling
335 mode, in continuous flow mode, the fitting improved slightly when applying a quadratic
336 function or an exponential function ($R^2 \geq 0.998$).

337 The two modes also distinguish themselves by the fact that with the continuous flow mode the
338 runs are shorter compared to the manual mode. The runs were set to 15 minutes closure for
339 the manual mode and to 7 minutes closure for the continuous flow mode. These times
340 included a maximum of 90 seconds equilibration time just after the sleeve was deployed to
341 allow the headspace to mix properly.

342 Runs 3 and 6 of the continuous flow mode were deliberately presented to display situations
343 where leakages from sleeves were occurring when placed on *Betula pendula* or *Pinus sylestris*
344 tree-stems (Fig. 6). In those cases, the CH_4 concentrations developed in a disordered way with
345 periods of increases immediately followed by sudden drops. These analytically monitored
346 leakages were confirmed when checking the chamber fitting on the stems.

347 The determination of the coefficient of variation of the root-mean-square error CV(RMSE),
348 often used to measure the relative differences between two populations of values, and which
349 was calculated between the linear fitted slopes and the non-linear fitted slopes, was higher in
350 the case of the manual sampling mode (0.69) as compared to the continuous flow mode (0.45).
351 In other words, the difference between the linear and non-linear fittings was 53% higher in the
352 manual mode as compared to the continuous mode. This went in parallel with the differences

353 between the average slope in the linear fitting and that from non-linear fitting which was 27%
354 higher with the manual sampling mode as compared to 18% with the continuous mode.

355

356 # 4 Discussion

357 ## 4.1 Semi-rigid sleeve construction

358 The semi-rigid sleeves are easy to assemble, lightweight, and can be locally sourced. The
359 sleeves could easily be assembled on-site following transportation. This allows for minimal
360 luggage or shipping space and low costs, a major asset in terms of logistics where remote
361 fieldwork is concerned. The PET or PC sheets were precisely cut in advance whereas the
362 framing with the Neoprene strips was done on-site. We made sure that all components were
363 not emitting CH_4, which might otherwise confound in-situ measurements. Nevertheless, the
364 raw materials are commonly available internationally, could be found on-site and likewise
365 tested. For small sleeves (stem diameters ≤ 15 cm) and middle-sized sleeves (stem diameters
366 ≤ 25 cm) the pre-shaped PET sheet can easily be constructed from soft drink PET bottles or
367 PC water-fountain tanks. Larger sleeves (stem diameters > 25 cm) can be built from flat PC
368 sheets as the curvature and volume stability of the chamber becomes less compromised with
369 larger stem diameters. Most important for the construction of the sleeves are the vertical
370 wedges that keep the sheet equidistant from the stem along the radial periphery of the sleeve.
371 The construction of a sleeve took about one hour and there was no requirement for specific
372 machine tools and no adhesives were needed, as the Neoprene bands used were adhesive
373 backed. For the production of large numbers of sleeve rectangular plastic sheets could be
374 thermoformed using a specially designed mould (Throne, 1996).

375 The average CH_4 mass losses (2.2-3.3 %) from the sleeves after 20 minutes of deployment
376 were two orders of magnitude greater as compared to the 0.038% mass loss after 30 minutes

of deployment reported by Hutchinson and Livingstone (2001) for a perfectly sealed chamber with a sole vent tube. Thereafter, our downscaled vent tube was proportioned to the CH_4 losses from the sleeves.

4.2 Calibration of the semi-rigid sleeves

All the chambers were reasonably precise (repeatable) in terms of total volume and the semi-rigid chambers (sleeves) performed equally compared to the rigid chambers. In terms of total volume inaccuracy, all chambers were below the threshold significance level of 5%. Moreover, the semi-rigid sleeves' total volume accuracy increased with increasing $S_c/V_{tot.}$ Nevertheless, getting good accuracy is a matter of calibration as biases can be subtracted from the original readings.

The average 33 cm^3 greater V'_{tot} values as compared to V_{tot} for the large sleeve (Supplement S1) can be attributed to the volume of the wedges that were also undergoing a compaction when deployed as the interior periphery gets compressed. This tiny volume correction was not inserted in formula 4 for the sake of simplicity and because the difference with the calibration was still below 5%.

We added a known amount of CH_4 instantaneously to the chambers and followed its decline and associated chamber permeability. Thereafter, we can be aware of how well the chambers are doing in keeping the considered gas but not how well they do in minimizing the errors associated with the gas exchange processes between stems and the chamber. For those errors we referred to recommendations from other studies, such as: ensuring air-mixing, venting, reducing closure times, reducing chamber volume and considering non-linear fitting (Christiansen et al., 2011; Hutchinson and Livingston, 2001; Juszczak, 2013; Pihlatie et al., 2013).

401

402 ### 4.3 Chamber permeability comparisons

403 A reasonable mechanistic explanation to the fact that both semi-rigid sleeves were on average
404 57% less permeable compared to the rigid chamber (Table 1) could come from the sleeve's
405 smaller proportion of air contact lines between inside and outside the chambers thereby
406 reducing opportunities for gas diffusion to occur. The difference in that proportion is similar
407 in order of magnitude to the difference in permeability (Supplement S2). Moreover, it is
408 possible that with an aging rigid chamber the permeability could increase faster than in the
409 case of an aging semi-rigid sleeve as the proportion of fixed contact lines could be exposed to
410 more cracks and unforeseen reduced air-tightness (Fig. 3, green lines).

411 This is also in line with the fact that for the same semi-rigid chamber design with the
412 increasing S_c-to-V_{tot} ratio, thus by increasing frame size, there is a concurrent decrease in the
413 proportion of contact lines as well as a concurrent decrease in permeability. The rigid
414 chamber had a much lower S_c-to-V_{tot} ratio when compared to the sleeves and showed the
415 greatest permeability. From our observations we can generalise the common trend found for
416 all chamber types by saying that the larger the total volume of a stem chamber is, for a given
417 gas exchange surface, the greater the expected permeability.

418 With the same logic and by considering the strong leverage effect of the concentration
419 gradient (ΔC) between inside and outside the chamber, the advantage of the larger rigid
420 chamber is that it keeps the concentration gradient more constant during the chamber
421 deployment and therefore minimizes the non-steady-state gas saturation effect of the closed
422 chamber system. However, this advantage loses its importance when semi-rigid sleeves are
423 connected to precise gas analysers with analytical frequencies of up to 10 Hertz as the
424 gradient effect can equally be minimized by reducing the closure times to a few minutes.

Additionally, by increasing the S_c-to-V_{tot} ratio by 6 fold compared to rigid chambers and by mixing the enclosed gas through the continuous flow circulation, we also avoided the problems associated with large volume chambers (Hutchinson and Livingston, 2001, 1993).

Nevertheless, the only non-compressible time factor is the sleeve's equilibration period; a 90 second period for the continuous air circulation to mix the entire headspace. This could be shortened by reducing the tube length, increasing the pump's flow-through or by installing a complementary fan if the sleeves were to be built much larger. In any case, the threshold time by which the sleeve headspace is mixed entirely can be monitored graphically while running every sample. Retrospectively, 90 seconds of equilibration, together with 3-minute closure time, conservatively characterised all replicates made for two different sleeve sizes (n=24).

4.4 Deployment in the field

As expected, deployment of the semi-rigid sleeve was very straightforward and could be operated by a single person. The fact that the sleeves had a natural tendency to curve (pre-shaped) allowed them to stay in place when initially placed around the stem. This gave the researcher free hands to attach the straps subsequently. The whole setup takes two minutes to install and swapping the sleeves between different stem heights was also done much more efficiently in comparison to the rigid chamber deployment.

In theory all stem sizes could be fitted, the only limitation comes from the stem texture and this is valid for both semi-rigid sleeves as well as rigid chambers. In some situations, the tree bark had large crevices and it was necessary to prepare the stem prior to attachment of the sleeves or rigid chambers. The preparation was made by filling the crevices with mastic or play dough in the shape of a frame before the chamber or sleeve could be sealed to the stem. In some other situations it was enough to increase the thickness of the sleeves to reduce the

449 percentage of uncertainty in the chamber volume (V_c). The impact of both crevices and
450 bumps could be assessed with distance measurements made on photos taken on one side of
451 the deployed sleeves.

452 Using five sleeve sizes it was possible to cover stem diameters ranging from 5 cm to 127 cm
453 at breast height (DBH). Moreover, in terms of weight the two sleeves we tested were
454 respectively 156 and 297 grams, compared to 3.3 kg for the rigid chamber. As a consequence,
455 the whole collection of sleeves fitted in a single backpack and was light to carry.

456 Under changeable conditions such as varying sunlight intensities we recommend that the
457 temperature inside and outside of the sleeve is measured, and to shade the sleeve. Otherwise,
458 these varying conditions may alter the gas exchange processes between the stem and the
459 atmosphere.

460 ### 4.5 Sampling modes and regression fits

461 In both cases, for manual sampling and continuous flow (Figs. 5 and 6), methane
462 accumulation rates were better fitted with non-linear functions (quadratic or exponential).
463 This confirms that the sleeve's closure system was sealing properly against the stems, as the
464 headspace concentration change of a closed non-steady-state chamber (static chamber) will
465 always remain non-linear and this is driven by the laws of diffusion (Hutchinson and
466 Livingston, 2001). For the semi-rigid sleeve, the difference between both the R^2 and the
467 slopes between the linear fitted and the non-linear fitted concentration changes were roughly
468 twice as small compared to those reported in the literature for soil chambers (Christiansen et
469 al., 2011; Hutchinson and Livingston, 2001; Juszczak, 2013; Pihlatie et al., 2013).

470 Furthermore, the impact of the manual syringe sampling on the pressure fluctuation in the
471 sleeve could be somewhat minimised by the fact that the chamber volume (V_c), where the
472 actual air mixing occurred, was increased by the additional dead volume added from the

analyser and tubing in continuous flow mode. Thus, the total volume ($V_{tot}=V_c+V_{dead}$) was increased as much as 76% with the smaller sleeve. With rigid soil chambers this aspect is often not mentioned as in those cases the dead volume is negligible compared to the large chamber volume. In our case, for the manual sampling, over a 15 minutes period, we drew 1.8% of the total volume from the larger sleeve (4 steps of 0.44%), which in terms of mass loss remains below the significance level of 5% and could be accounted for if more accuracy is needed. Although the repeated gas sampling minimises somewhat the pressure build up, recent studies have recommended avoiding manual sampling as much as possible because of associated pressure fluctuations (Christiansen et al., 2011; Juszczak, 2013).

The coefficient of variation of the root-mean-square error CV (RMSE) gave 53% higher coefficients for the manual sampling mode compared to the continuous flow mode thus indicating that the discrepancy between the linear fitting and the non-linear fitting is higher for the manual sampling mode. Moreover, as reported by some authors, fluxes calculated using linear fitting together with non-steady state chambers could be underestimated by as much as 40% (Christiansen et al., 2011; Pihlatie et al., 2013; Kutzbach et al., 2007). In our case, the underestimation was 27% for manual sampling mode and 18% for the continuous flow mode. As a consequence we would recommend using non-linear fitting (quadratic or exponential) together with manual sampling of the semi-rigid sleeves. In continuous flow mode, it is better to reduce the closure times as much as possible if planning to use linear fitting for greater simplicity. Both measures will contribute to improving line-fitting and estimating CH_4 accumulation rates.

5 Conclusions

Although all chamber types performed well, the semi-rigid design had numerous benefits including reduced gas permeability and an optimal S_c-to-V_{tot} ratio. Furthermore, they can be easily constructed and transported in multiple sizes, are extremely light, cheap to build and fast to deploy. As an example, in three of our tropical campaigns it was possible to carry a complete collection of semi-rigid sleeves in a single backpack. The collection covered the sampling of all ecosystem stem-sizes. Alternatively, we could also build the chambers on-site after prior testing of the compounds for background emissions. The PET and PC sheets of the sleeves are sturdy and lasted the duration of the campaigns, while the closed-cell Neoprene strips could be used for several weeks in the field before they needed to be replaced.

Connecting the sleeves in continuous flow mode to fast and precise laser-spectroscopic gas analysers (CRD or OA-ICOS technologies) enables the combined analysis and air mixing of the sleeve's enclosed volume, as well as reducing the closure periods to no-more than three minutes, making linear fitting from initial rates less problematic. To ensure optimal accuracy of the concentration measurements, it is best to calibrate each individual sleeve's total volume by diluting a standard gas in the entire setup (chamber, connectors, tubes and analyser) prior to starting a measurement programme.

Finally, to make good estimates of the global importance of tree-stem CH_4 emissions, it is essential to make measurements that cover all types of trees (species and morphotypes) present within the often remote ecosystems explored. This necessitates great adaptability in the chamber sizing and transport logistics. The semi-rigid sleeves meet these requirements without compromising the quality of the data collected.

Acknowledgments

519 We would like to thank the landscape biogeochemistry group at SLU Umeå for giving us
520 access to their workshop and laboratory. We would also like to thank Dr Róbert Blaško for
521 logistical help. This work was supported by Natural Environment Research Concil (NERC)
522 grant number NE/J010928/1 and AXA Research Fund, both to VG.

523

524 **References**

525 Baird, A. J., Stamp, I., Heppell, C. M., and Green, S. M.: CH_4 flux from peatlands: a new
526 measurement method, Ecohydrology, 3, 360-367, 10.1002/eco.109, 2010.

527 Bortoluzzi, E., Epron, D., Siegenthaler, A., Gilbert, D., and Buttler, A.: Carbon balance of a
528 European mountain bog at contrasting stages of regeneration, New Phytol., 172, 708-718,
529 10.1111/j.1469-8137.2006.01859.x, 2006.

530 Christiansen, J. R., Korhonen, J. F. J., Juszczak, R., Giebels, M., and Pihlatie, M.: Assessing
531 the effects of chamber placement, manual sampling and headspace mixing on CH_4 fluxes in a
532 laboratory experiment, Plant Soil, 343, 171-185, 10.1007/s11104-010-0701-y, 2011.

533 Fick, A.: Ueber Diffusion, Ann. Phys-Leibzig, 170, 59-86, 10.1002/andp.18551700105, 1855.

534 Gauci, V., Gowing, D. J. G., Hornibrook, E. R. C., Davis, J. M., and Dise, N. B.: Woody stem
535 methane emission in mature wetland alder trees, Atmos. Environ., 44, 2157-2160,
536 10.1016/j.atmosenv.2010.02.034, 2010.

537 Hari, P., Nygren, P., and Korpilahti, E.: Internal circulation of carbon within a tree, Can. J.
538 Forest Res., 21, 514-515, 10.1139/x91-069, 1991.

539 Hutchinson, G. L., and Livingston, G. P.: Use of chamber systems to measure trace gas fluxes,
540 in: Agricultural Ecosystem Effects on Trace Gases and Global Climate Change, edited by:
541 Harper, L. A., Mosier, A. R., Duxbury, J. M., Rolston, D. E., Peterson, G. A., Baenziger, P. S.,

542 Luxmoore, R. J., and Kral, D. M., American Society of Agronomy/Crop Science Society of
543 America/Soil Science Society of America, Madison, WI, USA, Madison, WI, 63-78, 1993.

544 Hutchinson, G. L., and Livingston, G. P.: Vents and seals in non-steady-state chambers used
545 for measuring gas exchange between soil and the atmosphere, Eur. J. Soil Sci., 52, 675-682.

546 IPCC: Climate Change 2007: The physical science basis. Contribution of working group I to
547 the fourth assessment report of the intergovernmental panel on climate change, Cambridge
548 University Press, Cambridge, UK and New York, USA, 996 pp., 2007.

549 Juszczak, R.: Biases in methane chamber measurements in peatlands, Int. Agrophys., 27, 159-
550 168, 10.2478/v10247-012-0081-z, 2013.

551 Kutzbach, L., Schneider, J., Sachs, T., Giebels, M., Nykanen, H., Shurpali, N. J., Martikainen,
552 P. J., Alm, J., and Wilmking, M.: CO_2 flux determination by closed-chamber methods can be
553 seriously biased by inappropriate application of linear regression, Biogeosciences, 4, 1005-
554 1025, 10.5194/bg-4-1005-2007, 2007.

555 Levy, P. E., Meir, P., Allen, S. J., and Jarvis, P. G.: The effect of aqueous transport of CO_2 in
556 xylem sap on gas exchange in woody plants, Tree Physiol., 19, 53-58,
557 10.1093/treephys/19.1.53, 1999.

558 LGR: Ultra-portable greenhouse gas analyzer user manual, model 915-0011, Los Gatos
559 Reaserch Inc., Mountain View, USA, 84 pp., 2013.

560 McKeen, L. W.: Film Properties of Plastics and Elastomers, Elsevier, Amsterdam, The
561 Netherlands, 408 pp., 2012.

562 Norman, J. M., Kucharik, C. J., Gower, S. T., Baldocchi, D. D., Crill, P. M., Rayment, M.,
563 Savage, K., and Striegl, R. G.: A comparison of six methods for measuring soil-surface
564 carbon dioxide fluxes, J. Geophys. Res., 102, 28771, 10.1029/97jd01440, 1997.

565 Ogulata, R. T., and Mavruz, S.: Investigation of Porosity and Air Permeability Values of
566 Plain Knitted Fabrics., Fibres & Textiles in Eastern Europe, 18, 71-75, 2010.

567 Pangala, S. R., Moore, S., Hornibrook, E. R. C., and Gauci, V.: Trees are major conduits for
568 methane egress from tropical forested wetlands, New Phytol., 197, 524-531,
569 10.1111/nph.12031, 2013.

570 Pihlatie, M. K., Christiansen, J. R., Aaltonen, H., Korhonen, J. F. J., Nordbo, A., Rasilo, T.,
571 Benanti, G., Giebels, M., Helmy, M., Sheehy, J., Jones, S., Juszczak, R., Klefoth, R., Lobo-
572 do-Vale, R., Rosa, A. P., Schreiber, P., Serca, D., Vicca, S., Wolf, B., and Pumpanen, J.:
573 Comparison of static chambers to measure CH_4 emissions from soils, Agr. Forest Meteorol.,
574 171, 124-136, 10.1016/j.agrformet.2012.11.008, 2013.

575 Pumpanen, J., Kolari, P., Ilvesniemi, H., Minkkinen, K., Vesala, T., Niinistö, S., Lohila, A.,
576 Larmola, T., Morero, M., Pihlatie, M., Janssens, I., Yuste, J. C., Grünzweig, J. M., Reth, S.,
577 Subke, J.-A., Savage, K., Kutsch, W., Østreng, G., Ziegler, W., Anthoni, P., Lindroth, A., and
578 Hari, P.: Comparison of different chamber techniques for measuring soil CO_2 efflux, Agr.
579 Forest Meteorol., 123, 159-176, 10.1016/j.agrformet.2003.12.001, 2004.

580 Rice, A. L., Butenhoff, C. L., Shearer, M. J., Teama, D., Rosenstiel, T. N., and Khalil, M. A.
581 K.: Emissions of anaerobically produced methane by trees, Geophys. Res. Lett., 37, L03807,
582 10.1029/2009gl041565, 2010.

583 Rusch, H., and Rennenberg, H.: Black alder (*Alnus glutinosa* (L.) Gaertn.) trees mediate
584 methane and nitrous oxide emission from the soil to the atmosphere, Plant Soil, 201, 1-7,
585 10.1023/a:1004331521059, 1998.

586 Ryan, M. G.: Growth and maintenance respiration in stems of *Pinus contorta* and *Picea*
587 *engelmannii*, Can. J. Forest Res., 20, 48-57, 10.1139/x90-008, 1990.

588 Subke, J. A., Reichstein, M., and Tenhunen, J. D.: Explaining temporal variation in soil CO_2
589 efflux in a mature spruce forest in Southern Germany, Soil Biol. Biochem., 35, 1467-1483,
590 10.1016/s0038-0717(03)00241-4|issn 0038-0717, 2003.

591 Terazawa, K., Ishizuka, S., Sakata, T., Yamada, K., and Takahashi, M.: Methane emissions
592 from stems of *Fraxinus mandshurica* var. *japonica* trees in a floodplain forest, Soil Biol.
593 Biochem., 39, 2689-2692, 10.1016/j.soilbio.2007.05.013, 2007.

594 Terazawa, K., Yamada, K., Ohno, Y., Sakata, T., and Ishizuka, S.: Spatial and temporal
595 variability in methane emissions from tree stems of *Fraxinus mandshurica* in a cool-
596 temperate floodplain forest, Biogeochemistry 123, 349-362, 10.1007/s10533-015-0070-y,
597 2015.

598 Teskey, R. O., and McGuire, M. A.: CO_2 transported in xylem sap affects CO_2 efflux from
599 *Liquidambar styraciflua* and *Plantans occidentalis* stems, and contributes to observed wound
600 respiration phenomena., Trees, 19, 357–362, 2005.

601 Throne, J. L.: Technology of Thermoforming, Technology of Thermoforming, Carl Hanser
602 Verlag GmbH & Co. KG, Munich, Germany, 898 pp., 1996.

603

604 **Figure captions**

605 **Figure 1**. Smaller semi-rigid stem sleeve attached to a stem. The plastic PET sheet (a) has
606 three imprinted circular rims (b) that ensured good stability and natural curvature of the sleeve.
607 The circumference of the sheet was framed with a 1.5 cm thick and 3 cm wide expanded
608 Neoprene strip (c) that sealed off the headspace located between the sheet and the stem. Inside
609 this volume there were two vertical wedges (d) that kept the sheet at equidistance from the
610 stem along the radial periphery of the sleeve. In its centre the sleeve was equipped with two

611 Snap-on rubbers with inserted three-way stopcocks (e) that were further connected to PVC
612 tubes that went from the sleeve to the Ultraportable Greenhouse Gas Analyser. A coiled vent
613 was placed in one corner of the sleeve (f) to regulate the pressure. The chamber was tightened
614 to the stem with the help of two straps that perfectly aligned on top of the horizontal strips.

615 **Figure 2**. The three steps of the semi-rigid stem sleeve deployment. To ensure a good contact
616 between the frame strips and the stem it was important to distribute the pressure of each strap
617 all around the frames' periphery when tightening the sleeve. Close to the centre two Snap-on
618 rubbers with inserted three-way stopcocks were pressed into the PET or PC plastic sheet.
619 These stopcocks were connected to the two PVC tubes that circulated air in a continuous flow
620 mode when connected to an Ultraportable Greenhouse Gas Analyser (UGGA).

621 **Figure 3**. Potential air contact path lines (chamber air versus ambient air) where gas diffusion
622 can occur; a comparison between the acrylic rigid cylinder approach and the semi-rigid sleeve
623 approach. The red lines represented the mobile contact lines that needed to be sealed properly
624 every time the chambers were deployed and where most of the losses were likely to occur.
625 The green lines represented the fixed contact lines which could have been leaking as a result
626 of twisting forces on the joints leading to cracks.

627 **Figure 4**. 2-D Layout for the chamber volume (V_c) calculation based on the stem diameter
628 (D_{stem}), the thickness of the chamber (T), the sector covered by the chamber (K) and the
629 volume of the wedges (V_{wedge}). Refer to the text for the volume calculations.

630 **Figure 5**. Contrasting methane concentration changes in the semi-rigid sleeve from enclosed
631 gas samples measured in a manual mode (syringe) from tree-stems. In the first six runs (top
632 quadrants) the concentration changes were regressed with a linear fit, while in the second set
633 of runs they were regressed with a quadratic fit (non-linear). All runs 1-6 were measured on
634 *Heisteria concinna* stems from a tropical lowland forest. The blue line corresponds to 95%

635 confidence intervals, *RMSE* = root-mean-square error, R^2 = coefficient of determination, *Y* =
636 methane concentration in ppmv.

637 **Figure 6**. Contrasting methane concentration changes in the semi-rigid sleeve from enclosed
638 gas samples measured in continuous flow mode (UGGA) from tree-stems. In the first six runs
639 (top quadrants) the concentration changes were regressed with a linear fit, while in the second
640 set of runs (bottom quadrants) they were regressed with quadratic fit (non-linear). Runs 1, 2, 3,
641 and 5 were made on *Betula pendula* stems, runs 4 and 6 were made on *Pinus sylvestris* stems,
642 runs 3 and 6 show the concentration responses in situations where the sleeves were leaking.
643 The blue line corresponds to 95% confidence intervals, *RMSE* = root-mean-square error, R^2 =
644 coefficient of determination, *Y* = methane concentration in ppmv.

645

Table 1. Chamber dimensions and mean permeabilities (*P*) determined, for each replicated chamber (n = 3), from the methane decline slope (*Slope*), the total chamber volume (V_{tot}), the initial concentration gradient between outside and inside (C_0-C_{atm}) and the gas exchange surface (S_c). *D* = metallic cylinder diameter, *L* = peripherical length of the enclosure, *H* = height, *T* = thickness, C_0 = initial enclosure concentration, C_{atm} = 1.8951 ppmv, R^2 = coefficient of determination of the decline regression, V_c = volume of the chamber, $V_{tot} = V_c + V_{dead}$, V_{dead} = dead volume of the analyser plus the tubes = 416 cm^3. Values in brackets represent the standard error of the mean (±SEM).

Enclosure type	***D* (cm)**	***L* (cm)**	***H* (cm)**	***T* (cm)**	**S_c (cm^2)**	**V_c (cm^3)**	**V_{tot} (cm^3)**	**C_0 (ppmv)**	***Slope* (mg m^{-3} s^{-1}) *10^{-4}**	**R^2**	***P* (m s^{-1}) *10^{-7}**
Small sleeve	15	25	16	1.5	330	550	966[a]	109.12 (2.00)	-21.40	0.930	8.30 (0.85)[d]
Large sleeve	15	30	24	1.5	594	990	1406[b]	71.43 (1.14)	-9.86	0.922	4.77 (0.64)[e]
Rigid chamber	15	28	30	6.5	1413	13165	13581[c]	9.58 (0.16)	-0.82	0.931	14.62 (1.86)[f]

Volume inaccuracies: [a] ±3.4%, [b] ±2.4%, [c] ±4.1%; Permeability inaccuracies*: [d] ±3.7%, [e] ±2.8%, [f] ±4.3%

*Calculated from the error propagation formula:

$$\frac{dP}{|P|} \leq \sqrt[2]{\left(\frac{dC}{|C|}\right)^2 + \left(\frac{dV}{|V|}\right)^2 + \sqrt[2]{dC^2 + dC_{atm}^2}} \cong \sqrt[2]{\left(\frac{dV}{|V|}\right)^2 + 2}$$

646

647

648

649

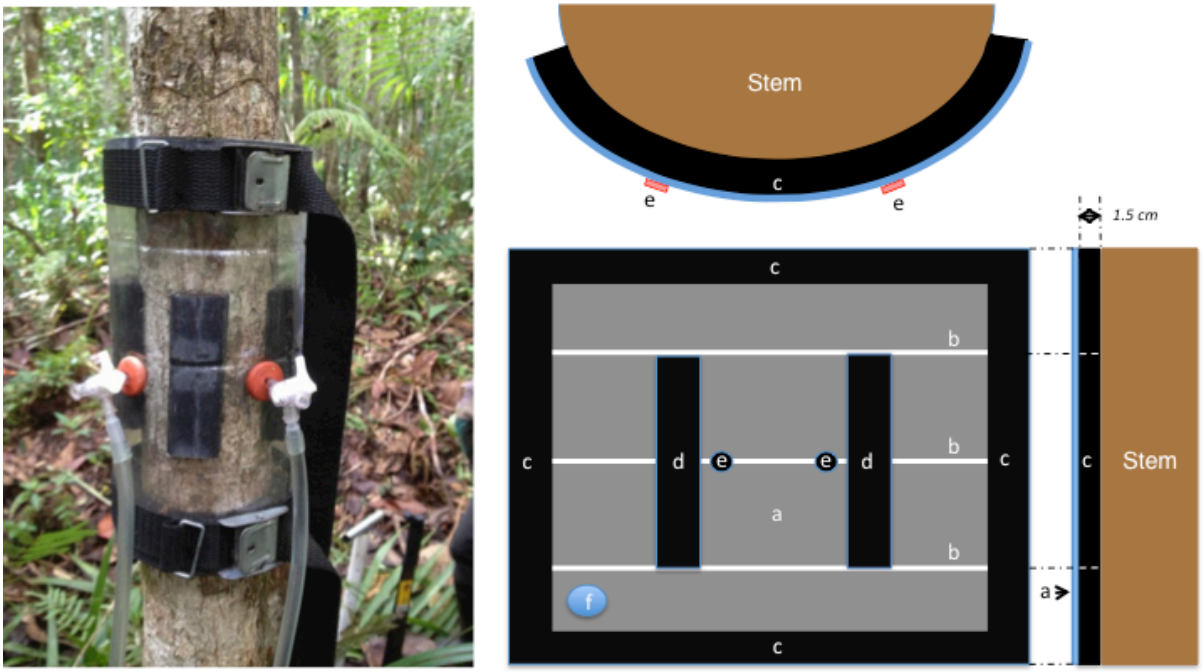

650

651 Fig01

652

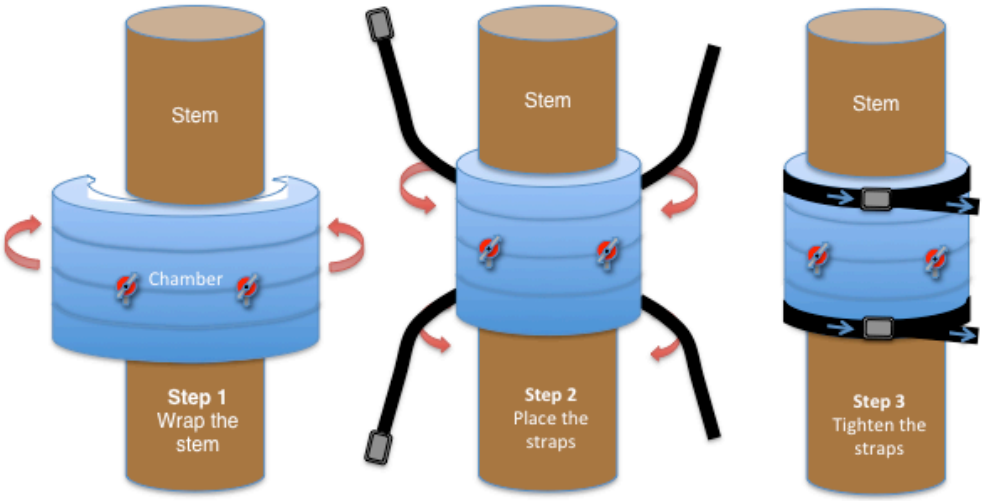

653

654 Fig02

655

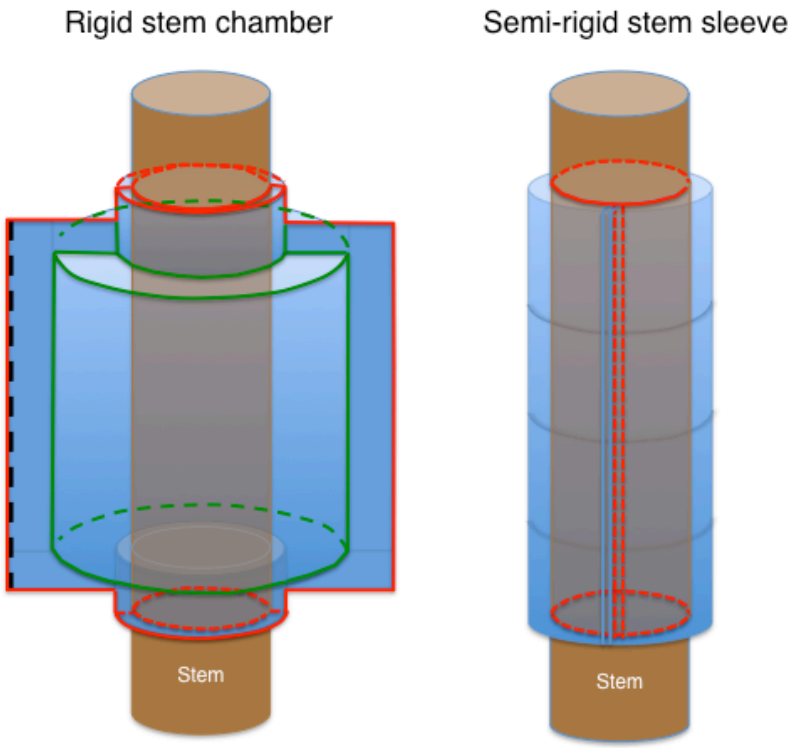

656

657 Fig03

658

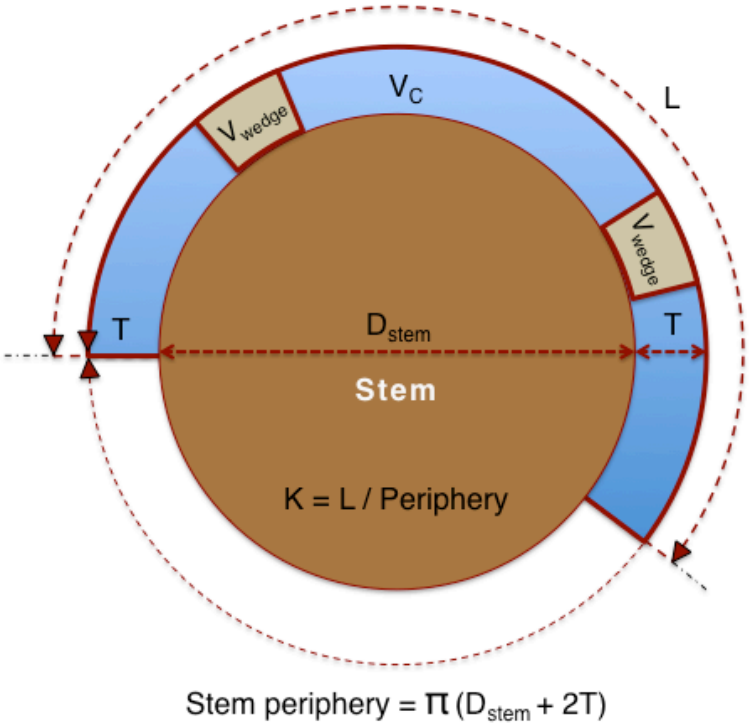

659

660 Fig04

661

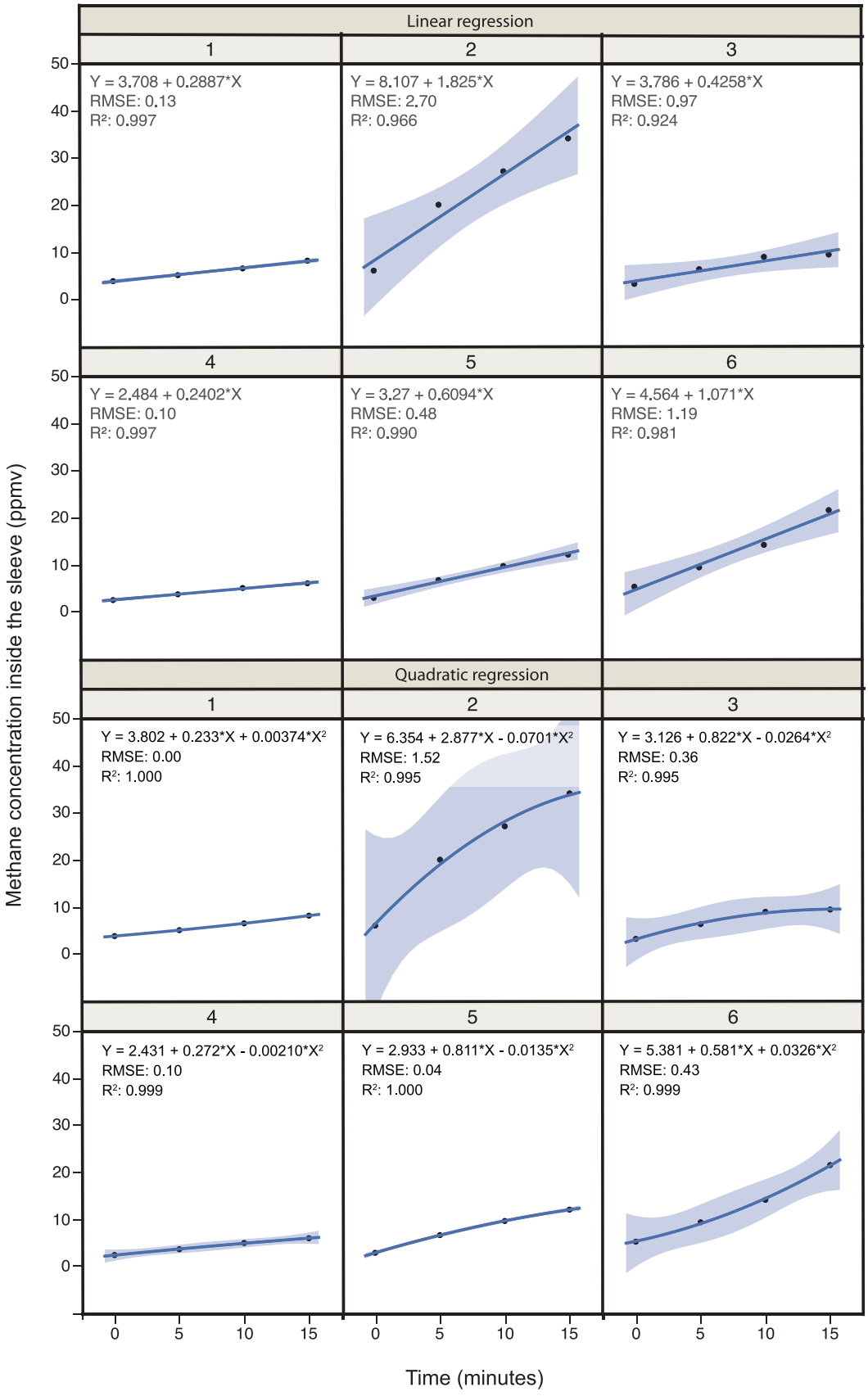

662

663 Fig05

664

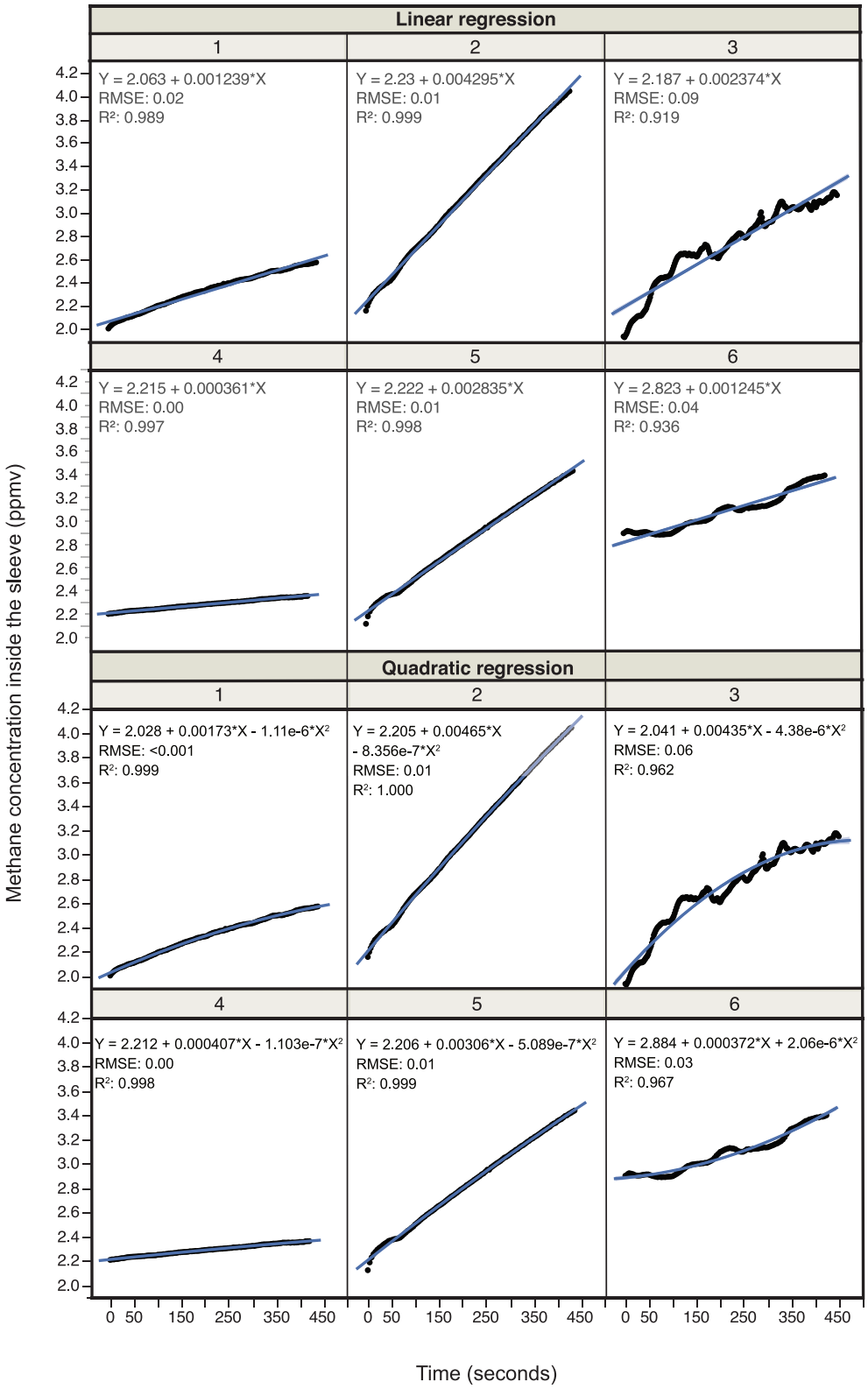

665

666 Fig06